Available online at www.sciencedirect.com
ScienceDirect
Polymer 47 (2006) 7813–7820
polymer
www.elsevier.com/locate/polymer

Variations of regular conformation structures in melt of syndiotactic polypropylene

Chunxiao Zheng [a,b], Xiuqin Zhang [a,b], Xia Dong [a], Ying Zhao [a], Zhigang Wang [a], Shannong Zhu [a], Duanfu Xu [a], Dujin Wang [a,*]

[a] *Beijing National Laboratory for Molecular Sciences, CAS Key Laboratory of Engineering Plastics and State Key Laboratory of Polymer Physics and Chemistry, Joint Laboratory of Polymer Science and Materials, Institute of Chemistry, Chinese Academy of Sciences, Beijing 100080, PR China*
[b] *Graduate School of Chinese Academy of Sciences, Beijing 100080, PR China*

Received 11 April 2006; received in revised form 22 June 2006; accepted 3 September 2006
Available online 25 September 2006

Abstract

Regular structures in polymer melt play important roles during crystallization and subsequently influence performances of polymer materials. In the present work, differential scanning calorimetry (DSC) and variable temperature Fourier transform infrared spectroscopy (VT-FTIR) were used to characterize the variations of regular structures in melt of syndiotactic polypropylene (sPP) during heating. It was found that during heating, the structural transition in sPP melt undergoes four stages: (1) destruction of long regular structures; (2) formation of short regular structures; (3) transition from short regular structures to isotropic state; and (4) isotropic state. These regular structures in sPP melt have distinct memory effects on the crystallization behaviors. By using Flory's RIS model, it was found that in final isotropic state, the most common conformers are *ttgg* and *tttt*, corresponding to helical and planar–zigzag conformations, respectively. These findings are helpful to deeply understand the essence of structures in sPP melt and microstructure variations during melting.

Keywords: Syndiotactic polypropylene; Melt state; Regular conformation structure

1. Introduction

Discovery of novel metallocene-based catalysts during 1980s has revolutionized polyolefin technology and offers attractive potential for controlled molecular mass and stereoregularity in chain structure. The ability to control configuration has sparked interests in structure studies of syndiotactic polypropylene (sPP), among which most structural characterizations have employed diffraction methods, yielding considerable insights into structures with long-range order. Based on the X-ray diffraction results, some basic concepts have been constructed: there are at least three crystalline forms in sPP, with *ggtt* conformations in helical form I, all-*trans* in form II, and $(g_2t_2g_2t_6)_n$ in form III [1–3]. The crystallization behavior of sPP, in fact, is more complicated with respect to the above mentioned three polymorphs, which have been intensively investigated by Lotz et al. and De Rosa et al. [2,3]. However, there is only little information regarding one of the crucial parts for sPP, namely, the conformation structures and its variation in the melt. The conformations in melt state consequently influence the morphology and property of solid sate, especially when sPP crystallizes at fast rates because sPP macromolecular chains have no enough time for the completion of crystallization.

In previous reports, small-angle neutron scattering (SANS) [4] and molecular dynamic simulations [5] have been used to study the effect of tacticity on the thermodynamic properties and molecular dynamics of polypropylene melts. The coil dimension and correlation time of sPP are found to be much higher than that of iPP in the melt. Rheological analysis

* Corresponding author. Tel.: +86 10 82616255; fax: +86 10 82612857.
E-mail address: djwang@iccas.ac.cn (D. Wang).

0032-3861/$ - see front matter © 2006 Elsevier Ltd. All rights reserved.
doi:10.1016/j.polymer.2006.09.005

[6,7] has also been applied to elucidate the variation of chain structures of sPP melt. It was found that the activation energy of flow, Newtonian viscosity and entanglement modulus of sPP are much higher than those of iPP. One hypothesis for the different rheological characteristics is that the sPP conformation structures are more difficult to be destroyed in melt. Because it is difficult to track changes of macromolecular conformation structures during melting by rheometer, rheological method can only qualitatively describe the apparent experimental phenomena, providing indirect proofs to the conformational variations in melt. Therefore, more precise and effective methods are needed to detect the conformation structure evolution in sPP melt. It will be the main aim of our present work.

In this paper, melting behavior of sPP was investigated by combination of differential scanning calorimetry (DSC) and variable temperature Fourier transform infrared spectroscopy (VT-FTIR). Interestingly, it was found that above the nominal melting temperature of sPP (128.4 °C, DSC datum at a heating rate of 2 °C/min), there exist two types of regular conformation structures, assigned as long helical and mixture of short helical and *trans*-planar conformations, respectively. With increasing temperature, long helical regular structure can be destructed and turned into short regular ones, which are present until the temperature is raised up to 200 °C. These findings are helpful to deeply understand melting of sPP and the essence of conformation structures in melt, which are crucial in affecting the reverse process of melting, i.e., crystallization and ultimate crystalline polymorphism of sPP.

2. Experimental part

2.1. Materials and sample preparation

The commercial sPP pellets were supplied by Atofina company with M_w of 1.46×10^5 g/mol and polydispersity of $M_w/M_n = 3.52$ (from GPC data). The melting temperature of 128.4 °C was obtained by DSC with a heating rate of 2 °C/min. The microstructure of sPP chains, determined by ^{13}C NMR spectroscopy, has the fraction of fully syndiotactic pentads [rrrr] of 81% and syndiotactic triads [rr] of 89%. The polymorphism of our sample is form I with a t_2g_2 conformation which is given by the wide-angle X-ray diffraction data. The sPP pellets were melt-pressed at 200 °C for 5 min and then compressed into films with thickness of ca. 50 μm, followed by quenching to room temperature.

2.2. DSC analysis

DSC measurements were carried out on a Perkin–Elmer DSC-7 differential scanning calorimeter. For the non-isothermal crystallization experiments, the sPP samples were first heated from room temperature to specific fusion temperature (T_f) at a heating rate of 2 °C/min and kept at T_f for 30 min. Subsequently, the sPP samples were rapidly quenched to 10 °C at a cooling rate of 100 °C/min, and during the cooling of scans DSC thermograms were recorded. The crystallization temperatures of the sPP samples with different T_f were determined from the crystallization peaks of primary crystallites. For the isothermal crystallization experiments, the sPP samples were first heated from room temperature at a heating rate of 2 °C/min to 140 °C, 170 °C, 190 °C, and 200 °C, respectively, and at each fusion temperature the samples were kept for different time periods to check the effect of holding time on the crystallization rate. Then the sPP samples were rapidly quenched to 90 °C at a cooling rate of 100 °C/min for isothermal crystallization.

2.3. VT-FTIR spectroscopic analysis

IR spectra were recorded on a Bruker Equinox-55 FTIR spectrometer with a MCT detector at a resolution of 2.0 cm^{-1} and 32 scans. The variable temperature experiments were carried out on a Perkin–Elmer's variable temperature device with KBr windows. In the heating process, the sample was heated from room temperature to 220 °C at a rate of 2 °C/min, and IR spectra were collected in the temperature range of 120–220 °C at a 2 °C interval before 160 °C and a 10 °C interval after 160 °C, respectively. Because melting of polymer crystals is also a relaxation process of macromolecular chains, to ensure the sufficient relaxation of sPP chains, the sPP samples were kept for 30 min at each test temperature before FTIR spectra were recorded. The retaining time (30 min) for IR spectrum collection at a certain temperature is in consistent with DSC measurement, so that the structural variations in sPP melt can be compared by using these two characterization methods. For comparison purpose, the sPP sample was cooled down from 220 °C to 120 °C at a rate of 2 °C/min, and IR spectra were collected at several selected temperatures.

3. Results and discussion

It is well known that the ordered structures in polymer melt have memory effects on crystallization behaviors, thus influencing the final mechanical properties of the materials [8–10]. More specifically, the remained ordered structures can act as nucleation precursors for polymer crystallization, and subsequently influence the crystallization rate and morphology. In general, the higher the regularity in melts, the less the free energy difference between crystalline domains and melts, and the easier the occurrence of crystallization. Since the sPP melts at specific fusion temperatures (T_f) have different ordering degrees, the corresponding crystallization behaviors might be different, unless there are no ordered structures remaining in melts. Based on the above basic thought, DSC study was performed to examine whether there exist such ordered structures in sPP melts or not, especially above its equilibrium melting temperature ($T_m^o = 142$ °C, obtained by using linear Hoffman–Weeks plot from DSC data).

It was found from Fig. 1 that the crystallization temperature (T_c) of sPP changes obviously with variation of T_f, suggesting that T_f influences T_c a lot. Plotting T_c as the function of T_f is shown in Fig. 2. It can be seen that T_c of sPP undergoes four stages with the increasing T_f: (1) $T_f < 166$ °C, T_c

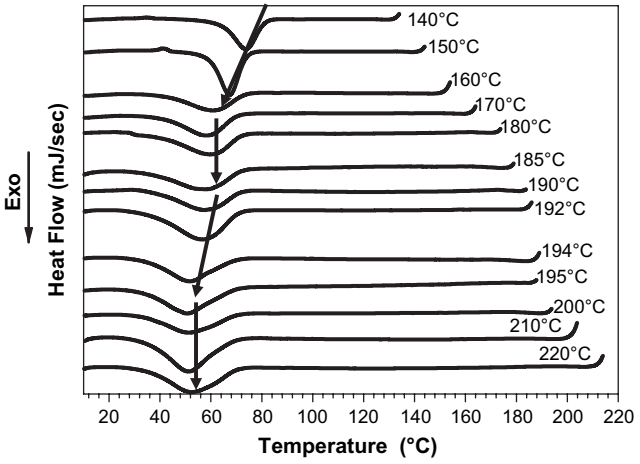

Fig. 1. DSC scanning curves of sPP during quenching at a cooling rate of 100 °C/min from melts formed by initially heating to different specific fusion temperatures (T_f) to 10 °C.

obviously shifts toward lower temperature; (2) $T_f = 166-184$ °C, T_c keeps about constant; (3) $T_f = 184-194$ °C, T_c shows more dramatic decreasing; (4) above $T_f = 195$ °C, T_c keeps almost constant. The above results are quite interesting. It is generally thought that T_c does not depend on T_f if there are no ordered structures in isotropic polymer melt. Herein we found that there are three distinct turning temperatures of 166 °C, 184 °C, and 194 °C for sPP crystallization, implying that sPP melts at different fusion temperatures possess different ordered structures or different conformation structures. As we will discuss later, these conformation structures include long and short conformational regular structures. The long conformational regular structures are originated from the regularly arranged polymer chains in crystalline domains, and exist only at the relatively low fusion temperatures; the short regular structures, i.e., the partially destructed regular polymer chains, however, persist to high T_f.

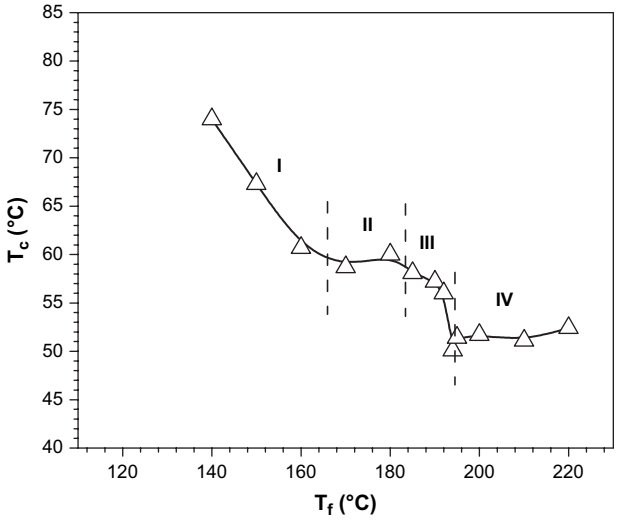

Fig. 2. Crystallization temperature (T_c) versus fusion temperature (T_f) for different sPP melts. Regions I: transition from long ordered structures to short ordered structures; II: short ordered structures; III: transition from short ordered structures to isotropic state; IV: isotropic state.

With increasing T_f in region I, long regular structures originating from melting of crystallites become short and the amount of long regular structures accordingly decreases obviously. Correspondingly, short regular structures increase and exist in certain temperature range (region II). Therefore, T_c of sPP obviously decreases until the amount of long regular structures reduces to undetectable quantity by DSC method. It is known that for sPP, above the nominal melting temperature of 128.4 °C, although the crystal lattices are destroyed, there still exist some residual memories for the former chain foldings, which are advantageous to the reversal to melting, i.e., the nucleation and growth for crystallization [11]. In the present work, it was observed that although almost all the long regular structures are destructed above 166 °C, there are short regular structures surviving in sPP melt below 184 °C. This hypothesis is further strengthened by the subsequent changes of T_c. When T_f exceeds 184 °C, T_c shows further dramatic decreasing with increasing T_f (region III), indicating a process of depletion of short regular structures in sPP melts. This depletion is accomplished till $T_f = 194$ °C, and afterwards sPP is assumed to be completely melted, resulting in constant crystallization temperature of 52 °C (region IV). Above 195 °C, sPP melt becomes isotropic, only including infusible heterogeneous nuclei originally presented in sPP resin, e.g., impurities and catalyst residues, etc. [11].

The above non-isothermal crystallization experiments give the evidence of ordered structures in sPP melt, and the isothermal crystallization results are described as below. It is known that the higher the regularity in melts, the quicker the isothermal crystallization will be, i.e., the shorter the crystallization half-time ($t_{1/2}$). In the isothermal crystallization experiments, the sPP samples were heated to four fusion temperatures, respectively, and at each fusion temperature, the sPP melts were kept for different time periods, then quenched to 90 °C for isothermal crystallization. In the isothermal crystallization process, the relative degree of crystallinity at time t, $X(t)$, could be calculated according to the following equation:

$$X(t) = \frac{\int_0^t \frac{dH}{dt} dt}{\int_0^\infty \frac{dH}{dt} dt} = \frac{\Delta H_t}{\Delta H_\infty} \quad (1)$$

where dH/dt is the rate of heat evolution; ΔH_t, the heat generated at time t, and ΔH_∞, the total heat generated up to the end of the crystallization process. From the equation, we can get an important parameter, i.e., the crystallization half-time ($t_{1/2}$), which is defined as the time taken from the onset of the crystallization until 50% completion.

Fig. 3 shows the development of the relative degree of crystallinity $X(t)$ with crystallization time t for the isothermal crystallization of sPP at 90 °C after melting for 50 min at different fusion temperatures. From Fig. 3, we can see that as the fusion temperature increases, the $t_{1/2}$ becomes longer, revealing that the degree of regularity in the melt decreases. The relationship among $t_{1/2}$, fusion temperature and different annealing time is summarized in Fig. 4. It is found that at 140 °C, although it is

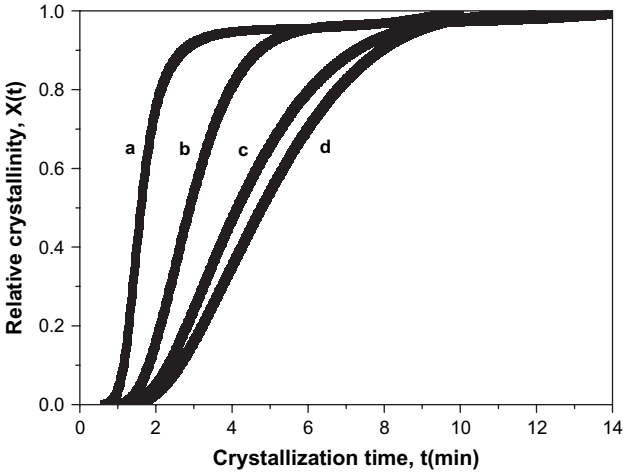

Fig. 3. Development of the relative crystallinity $X(t)$ degree of sPP with crystallization time t at 90 °C after melting for 50 min at different fusion temperatures: (a) 140 °C, (b) 170 °C, (c) 190 °C, and (d) 200 °C.

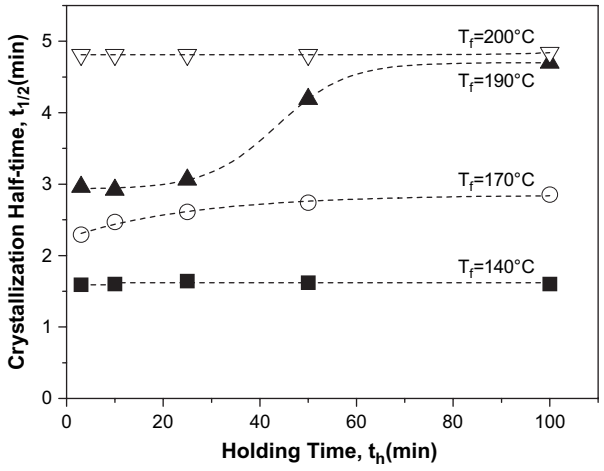

Fig. 4. Effects of fusion temperature (T_f) on the isothermal crystallization half-time of sPP melts, which were held for different time periods at each fusion temperature.

above the nominal melting temperature of sPP (128.4 °C), a long annealing time cannot destroy the ordered structures in sPP melt, which is reflected by the small changes of $t_{1/2}$ with the increase of annealing time. This means that the destruction of the ordered structures in sPP melt at 140 °C might need a relatively long time. At 170 °C and 190 °C, there is an obvious increase of $t_{1/2}$ with the increase of annealing time, implying that the ordered structures in sPP melt decrease with the increase of annealing time. Especially when the annealing time goes up to 100 min at 190 °C, the $t_{1/2}$ is almost the same as that of 200 °C. At 200 °C, even a short annealing time will destroy most of the ordered structures in sPP melt, therefore, the $t_{1/2}$ does not change largely with the increase of annealing time.

Polymorphism phenomena exist in solid states of sPP. In general, sPP has four crystalline modifications and one mesomorphic phase, which can transform from one modification to another by changing crystallization conditions or stressing/relaxing [12–14]. Four crystal forms correspond to different chain conformation structures, more specifically, crystalline form I and form II adopt $(t_2g_2)_n$ helical conformation [15–17], whereas form III and form IV present chains in *trans*-planar zigzag and $(t_6g_2t_2g_2)_n$ conformations, respectively [18,19]. Although extensive investigations have been performed on crystallization behaviors of sPP, much less information is available in literatures about the microstructures of sPP melts. In order to clarify the ordered structures detected by DSC in sPP melts, VT-FTIR spectroscopy was applied to follow the microstructure changes during melting of sPP. According to Zerbi et al. [20], the infrared spectra of semi-crystalline polymers can be classified into four groups related to various molecular structures: conformational band, stereoregularity band, regularity band and crystallinity band, among which regularity bands are attributed to the intramolecular coupling of oscillations of various groups [20–22]. The variations of regularity bands can provide important information about evolution of the ordered structures during melting. For sPP, there are mainly two types of regularity bands, assigned to helical form and planar–zigzag conformation, respectively. In the mid-infrared region, 868, 977, and 1005 cm^{-1} bands are assigned to helical form of sPP, while 963 cm^{-1} band is related with the planar–zigzag conformation [23–26]. More specifically, 963 cm^{-1} band is associated with the presence of short planar–zigzag conformation, which mainly exists in the amorphous phase [27]. To quantitatively compare conformational variations in melt, 1153 cm^{-1} band of asymmetric deformation vibration of methyl group in sPP was chosen as an internal standard, which is insensitive to conformational transition [28].

Fig. 5 shows a series of sPP spectra within the range of 1200–850 cm^{-1} during heating at a rate of 2 °C/min. It was observed that with increasing temperature, intensities of the bands of helical conformation at 1005, 977, and 868 cm^{-1}, and of planar–zigzag conformation at 963 cm^{-1} demonstrate

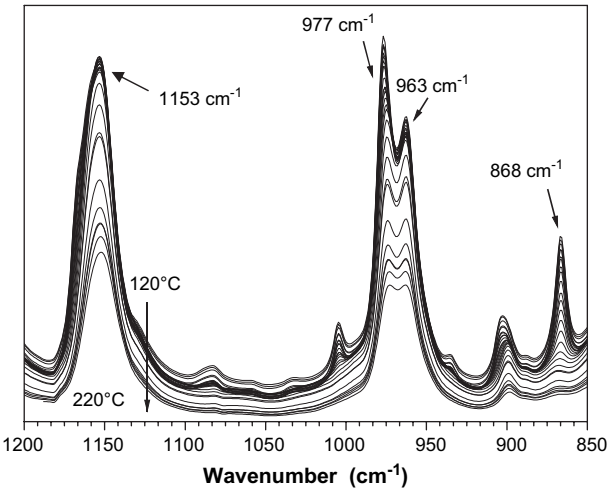

Fig. 5. FTIR spectra of sPP during heating at a rate of 2 °C/min. At each testing temperature, the samples were kept for 30 min to ensure sufficient chain relaxation. IR spectra were collected in the temperature range of 120–220 °C at 2 °C interval before 160 °C and 10 °C interval after 160 °C, respectively.

strong temperature dependence. The intensities of helical conformation bands manifestly decrease with increasing temperature, though that of the planar–zigzag conformation shows more complicated variations. Variations of the conformational bands can, to some extent, represent the changes of the ordered structures in polymer melts [29]. In order to quantitatively follow the changes of ordered structures in sPP melts, evolutions of the relative intensity ratios of 977, 963, and 868 cm^{-1} bands to 1153 cm^{-1} band during heating are shown in Fig. 6, respectively. As T_f is higher than T_m (128.4 °C), a large loss of intensity ratio of 868 cm^{-1} band was observed, indicating an abrupt change in the concentration of helical regularity during melting. This process lasts till 166 °C. It can be deduced that 868 cm^{-1} band corresponds to long ordered structures of helical conformation in sPP melt, which exist above T_m but attenuate quickly with increasing temperature until complete disappearance at 166 °C. This process is in good consistence with DSC trace (see Fig. 1), i.e., both FTIR and DSC results indicate that long ordered structures of helical conformation in sPP melt decrease almost linearly with T_f before 166 °C. Similar phenomenon has also been observed in iPP melt, in which the ordered structures at this stage were considered as a partially ordered melt, with the degree of ordering much lower than its crystalline state, but higher than the unperturbed melts [20,29,30].

Opposite to 868 cm^{-1} band, the intensity ratio of 963 cm^{-1} band increases slowly after sPP crystals are melted at about 128 °C, implying that more planar–zigzag structures are formed. The possible explanation is that upon heating the long ordered structures are partially destructed some of which are changed into short planar–zigzag conformations. This infers that short planar–zigzag structures increase at the cost of destruction of long regular helical structures. The short planar–zigzag structures can be stable above $T_f = 182$ °C. Above 182 °C, intensity ratio of 963 cm^{-1} band gradually decreases with increasing temperature until reaching a constant value at about 210 °C, above which sPP melt is believed to become completely isotropic.

As aforementioned, 977 cm^{-1} band can also be used to represent the helical forms of sPP. It is interesting to note that before 152 °C, intensity ratio of 977 cm^{-1} band decreases with increasing temperature, which is similar to 868 cm^{-1} band, but after that, the variation of intensity ratio of 977 cm^{-1} band is more similar to that of 963 cm^{-1} band. It infers that the 977 cm^{-1} band stands for not only long regular helical conformation structures but also short helical structures. The decrease of intensity ratio of 977 cm^{-1} band before 152 °C stands for destruction of long ordered helical structures. Above 152 °C, as long ordered helical structures are destroyed and turned into short ordered structures, including short helical forms too, intensity ratio of 977 cm^{-1} band gently increases with increasing temperature. Above 182 °C, a partial of short ordered structures in sPP melt are turned into isotropic state, causing further decrease of intensity ratio of 977 cm^{-1} band. As temperature is raised above 210 °C, the intensity ratio becomes constant, implying accomplishment of transition from short ordered structures to isotropic state in sPP melt. It should be pointed out that the transition temperatures are not exactly the same for DSC measurement (195 °C) and FTIR spectroscopy (210 °C), it might due to the different sensitivities between FTIR spectroscopy and DSC measurement, or due to the different thermal history of various melt states.

From the above, we can see that the ordered structures in sPP melt change a lot during heating. These ordered structures especially long ordered ones have been considered to originate from initial crystalline domains. To examine whether these ordered structures can be recovered from final state during cooling, FTIR spectra were collected during cooling as shown in Fig. 7. The comparing plots of intensity ratios for specific IR bands during heating and cooling are shown in Fig. 8. For long regular conformational band at 868 cm^{-1}, heating leads to an obvious decrease of intensity ratio until final disappearance, while cooling from 220 °C to 120 °C does not show any obvious influence on intensity ratio of 868 cm^{-1} band. As 868 cm^{-1} band mainly originates from crystalline part of sPP,

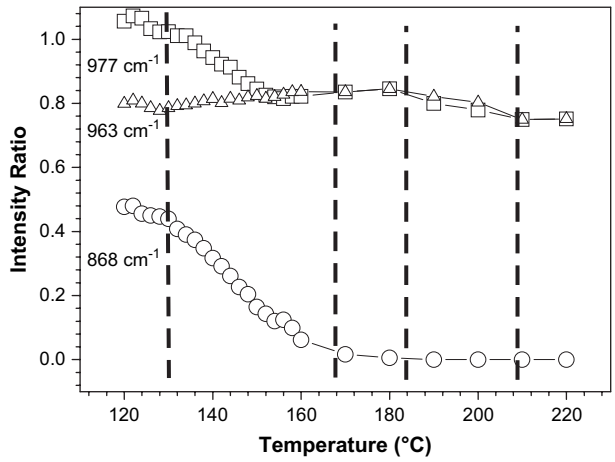

Fig. 6. Evolution of intensity ratios for different conformational bands of sPP during heating from 120 °C to 220 °C.

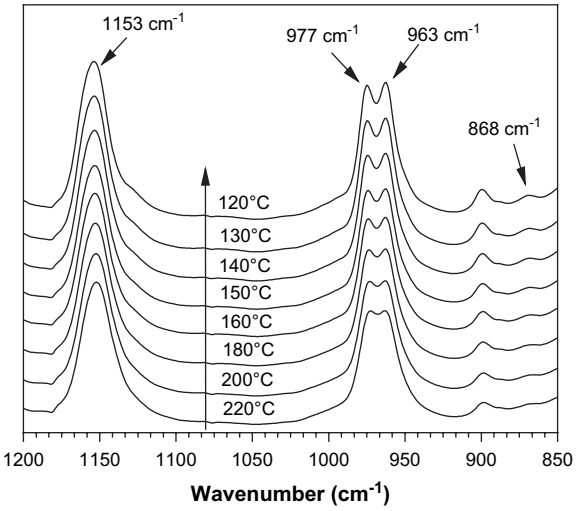

Fig. 7. FTIR spectra of sPP during cooling from 220 °C to 120 °C at a rate of 2 °C/min.

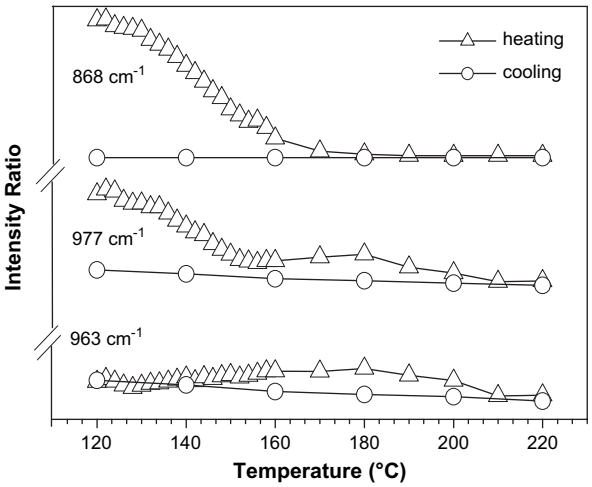

Fig. 8. Comparison of evolutions of intensity ratios for different conformational bands of sPP between heating and cooling of sPP.

the unchanged intensity of this peak within the experiment time indicates that the crystallization does not occur in the temperature region of 120–220 °C. Therefore, the relative intensity of 868 cm^{-1} band cannot reach the original intensity value in the heating run. The relative intensities of the bands 977 and 963 cm^{-1}, which represent mainly short regular structures, also show obvious differences between the heating and cooling processes. In the cooling process, the intensity ratios of 977 and 963 cm^{-1} bands keep almost constant above 150 °C, and increase slightly below 150 °C. The reason is that the short ordered structures mainly originate from the amorphous part of sPP in the cooling process. Above 150 °C, little amount of short ordered structures cannot recover from the melt, due to the erasing of the thermal history of sPP sample. As temperature decreases from 150 °C to 120 °C, the short ordered structures are feasible to form from the amorphous melt, thus the relative intensities of these two bands gradually increase, especially the 963 cm^{-1} band, which almost recovers to the same relative intensity as the starting value in the heating process.

The above results indicate that at 220 °C sPP melt is isotropic and it takes long time for sPP to nucleate during crystallization because long ordered structures cannot be recovered rapidly during cooling. The result validates also that long ordered structures originate from crystalline domains in sPP during heating. We thus deduce that formation of short ordered structures during heating mainly comes from destruction of long ordered ones. The significant difference of intensity ratios between heating and cooling affirms that the crystallization peak temperature changes in Figs. 1 and 2 are mainly due to variations of regular conformation structures in sPP melts during heating.

To summarize the results from the measurements by DSC and FTIR spectroscopy, it was clear that sPP undergoes a four-stage process during heating: firstly, below 166 °C, long ordered helical structures in sPP melt are gradually destroyed and turned into short ordered structures; secondly, in the temperature range of 166–184 °C, short ordered structures including short helical and planar–zigzag forms are maintained; thirdly, short ordered structures in sPP melt change into isotropic state from 184 °C to 194 °C (DSC) or 210 °C (FTIR), with the variation of transition temperature due to different sensitivities of the experimental methods; finally, sPP melt becomes completely isotropic. By combining DSC and FTIR results, the correlation between melting and conformational structures can be successfully established. Fig. 9 distinctly describes the structural transitions for sPP during melting. In solid state (Fig. 9a), sPP chains are well packed in crystalline domains, which are origins of long regular helical structures. Here we note that sPP chains in amorphous domains are not emphasized. Above melting temperature, long helical structures are deformed and destructed gradually. At the same time, short ordered structures are formed with some of them adopting helical conformations and the others adopting planar–zigzag conformations (Fig. 9b). As temperature continuously increases, long ordered structures are mostly turned into short ones (Fig. 9c). The regularity of sPP melts further decreases with increasing temperature, and eventually only were random coils of sPP chains kept in melt (Fig. 9d). Although we have given out schematic structure transitions of sPP during heating in Fig. 9, the scales for each ordered structures have not been determined by an appropriate experimental method. Other experimental techniques or theoretical study is still necessary for further understanding the ordered structures in melts.

It was observed that both DSC and FTIR techniques cannot detect the structures in sPP melt above 210 °C. However, it is interesting to know which kind of conformers that sPP macromolecular chains prefer to adopt in isotropic state. An effective method is to calculate the conformational probability by using Flory's polypropylene model [31]. There are five rotational isomeric states (RIS) in this model, i.e., *trans* 1 (*t*), *trans* 2 (*t**), *gauche* 1 (*g**), *gauche* 2 (*g*), and *gauche* 3 (*g*′). Fig. 10 illustrates the first-order interactions of the five states.

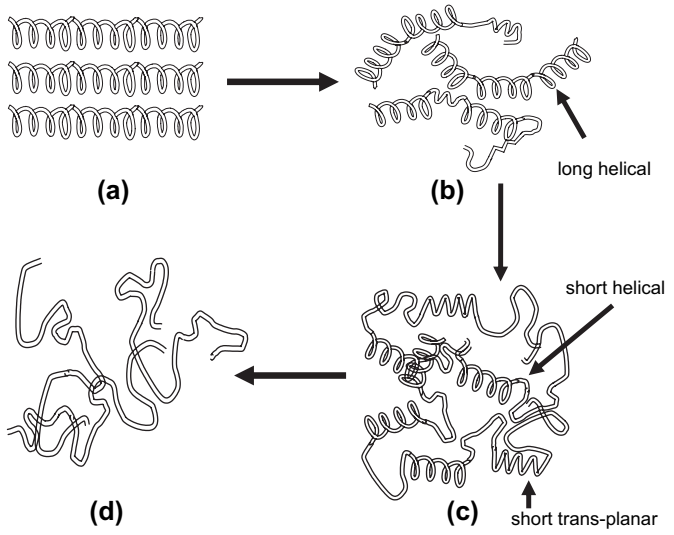

Fig. 9. Schematic structural transitions during heating of sPP: (a) crystalline domains, (b) destructed long ordered structure, (c) short ordered structure, and (d) isotropic state.

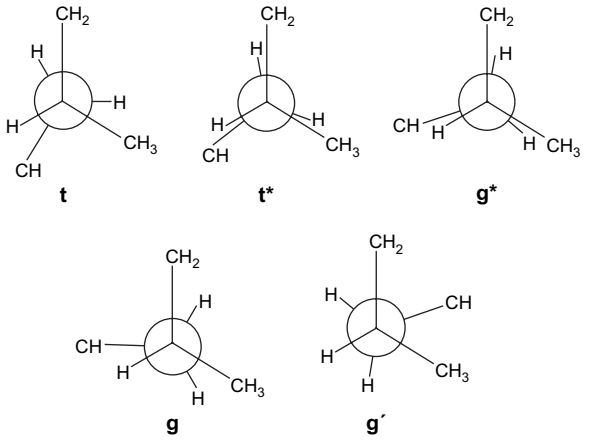

Fig. 10. Five-state rotational isomeric state model for sPP [31].

Herein we chose sPP melt at 210 °C as an example. The possible conformers for four successive main chain bonds of sPP were computed at this temperature. To apply the rotational isomeric state model to build asymmetric chains, each chiral center must be specified in its meso-form or racemic-form [31,32]. For a syndiotactic polymer in racemic-form, appropriate statistical weighting matrices are defined as:

$$U' = \begin{bmatrix} 1 & 1 & 1 & 1 & 1 \\ 1 & 1 & 1 & 1 & 1 \\ 1 & 1 & 0 & 0 & 1 \\ 1 & 1 & 0 & 0 & 1 \\ 1 & 1 & 1 & 1 & 0 \end{bmatrix}, \quad U''_{\mathrm{r}} = \begin{bmatrix} \eta^2 & 0 & \eta\omega^* & 0 & 0 \\ 0 & 0 & 0 & \omega^* & \tau\omega^* \\ \eta\omega^* & 0 & 0 & 0 & \tau\omega^* \\ 0 & \omega^* & 0 & 1 & 0 \\ 0 & \tau\omega^* & \tau\omega^* & 0 & 0 \end{bmatrix}$$

where matrix U' stands for the inter-dyad bond pair, i.e., the pair of bonds flanking the substituted carbon center; U'_{r} is for the dyad pair between two successive substituted carbon centers. η, ω^*, τ are the three statistical weight parameters, evaluated as functions of temperature from partition functions and average energies computed for each of the domains, which are shown in Eqs. (2)–(4), respectively:

$$\eta = 1.05\exp(-70/\mathrm{R}T) \tag{2}$$

$$\omega^* = 0.90\exp(-1500/\mathrm{R}T) \tag{3}$$

$$\tau = 0.4\exp(-500/\mathrm{R}T) \tag{4}$$

In the above equations, η and τ are the first-order interactions, and ω^* represents all second-order interactions between the pairs of groups, CH_2 and CH_2, CH_3 and CH_2, and CH_3 and CH_3, separated by four C–C bonds.

The chain conformation partition function for a syndiotactic polymer chain is represented by:

$$Z = J\left(U'U''_r\right)^{(n-2)}J^* \tag{5}$$

where $J = [1,0,0,0,0]$, $J^* = [1,1,1,1,1]'$, and n corresponds to bond number in computation. Here we chose 64 main chain bonds for computation.

Table 1
Possible conformers in sPP melt (210 °C) based on Flory's five-state RIS model

Conformers	Expectation
ttgg	0.2608
tttt	0.2197
ttgt + ttg′t**	0.1076
*ttg*t + ttg*t′*	0.1048
tttg + ttt*g*	0.0972
*ttg*g′ + ttg′g**	0.0316

To simulate random chains under isotropic state, it is necessary to apply the conditional probability matrices for each backbone conformer. Each element in the conditional probability matrix, P_{lm}, is obtained from the following equation:

$$P_{\mathrm{lm}} = \frac{J^*\left(\prod_{i=2}^{j-1}U_i\right)\tilde{U}_j\prod_{k=j+1}^{n-1}U_kJ}{Z} \tag{6}$$

where $\tilde{U}_j$ is obtained by replacing all the elements of matrix U_j in the partition function Z with zero, except for element U_{lm}, which remains unchanged.

By this method, the probabilities of specific conformers of sPP at 210 °C can be calculated. Table 1 shows that the main conformers in sPP melt at 210 °C are *ttgg* and *tttt*, corresponding to helical and *trans*-planar zigzag structures, respectively. It was also found that the content of *ttgg* conformer is slightly higher than that of *tttt*, indicating that in isotropic state, *ttgg* is the most common conformer in sPP melt. The existence of both *ttgg* and *tttt* conformers might be the motivation for the formation of short helical and *trans*-planar conformations in the temperature range of 160–200 °C (Fig. 6, regions II and III). Therefore, the computation results indirectly support the DSC and FTIR data.

4. Conclusions

By combination of DSC, FTIR spectroscopy and Flory's RIS model, the microstructures in sPP melt during heating have been well investigated. The following conclusions have been drawn:

(1) In sPP melt, multi-scaled regular structures exist in a wide temperature range from 130 °C to 210 °C.
(2) Above the nominal melting temperature of sPP (128.4 °C), the regular structures in sPP melt experience two structural transitions, one of which is the destruction of long regular helical conformations, and the other is the change from short helical or *trans*-planar conformation to isotropic state.
(3) These regular structures in sPP melt have memory effect on the crystallization behavior. The higher the regularity is in melts, the easier the occurrence of crystallization.
(4) In isotropic state of sPP melt, the most common conformers are proved to be *ttgg* and *tttt*, corresponding to basic elements of helical and *trans*-planar zigzag conformations, respectively.

Acknowledgements

The authors acknowledge the financial support from National Natural Science Foundation of China (NSFC, Grant Nos. 50290090, 20490220, and 10590355). ZG Wang acknowledges the financial support from ''Hundred Young Talents'' Program of Chinese Academy of Sciences.

References

[1] Nattta G, Peraldo M, Allegra G. Makromol Chem 1964;75:215.
[2] Auriemma F, Born R, Spiess HW, De Rosa C, Corradini P. Macromolecules 1995;196:4011.
[3] Lovinger AJ, Lotz B, Davis DD. Polymer 1990;31:2253.
[4] Jones TD, Chaffin KA, Bates FS. Macromolecules 2002;35:5061.
[5] Antoniadis SJ, Samara CT, Theodorou DN. Macromolecules 1999;32:8635.
[6] Tapadia PS, Joshi YM, Lele AK, Mashelkar RA. Macromolecules 2000;33:250.
[7] Elena R, Maria EM, Anton S, Begoña P. Macromol Rapid Commun 2004;25:1314.
[8] Ziabickia A. Colloid Polym Sci 1994;272:1027.
[9] Alfonso GC, Ziabickia A. Colloid Polym Sci 1995;273:317.
[10] Uehare H, Yamazaki Y, Kanamoto T. Polymer 1996;37:57.
[11] Supaphol P, Spruiell JE. J Appl Polym Sci 2000;75:337.
[12] Zhang XQ, Zhao Y, Shi HF, Dong X, Wang DJ, Han CC, et al. J Polym Sci Part B Polym Phys 2005;43:2924.
[13] Parthasarathy G, Sevegney MS, Kannan RM. Polymer 2005;46:6335.
[14] Gatos KG, Kandilioti G, Galiotis C, Gregoriou VG. Polymer 2004;13:4453.
[15] De Rosa C, Auriemma F, Corradini P. Macromolecules 1996;29:7452.
[16] De Rosa C, Auriemma F, Vinti V. Macromolecules 1998;31:7430.
[17] Loos J, Buhk M, Petermann J, Zoumis K, Kaminsky W. Polymer 1996;37:387.
[18] Chatani Y, Maruyama H, Noguchi K. J Polym Sci Part C Polym Lett 1990;28:393.
[19] Chatani Y, Maruyama H, Asanuma T, Shiomura T. J Polym Sci Part B Polym Phys 1991;29:1649.
[20] Zerbi G, Ciampelli F, Zamboni V. J Polym Sci 1963;C7:141.
[21] Miyamoto T, Inagaki H. J Polym Sci 1969;A27:963.
[22] Kissin YV. Adv Polym Sci 1975;15:92.
[23] Corradini P, Natta G, Ganis P, Temussi PA. J Polym Sci 1967;16:2477.
[24] Guadagno L, D'Aniello C, Naddeo C, Vittoria V. Macromol Rapid Commun 2001;21:104.
[25] Vittoria V, Guadagno L, Comotti A, Simonutti R, Auriemma F, De Rosa C. Macromolecules 2000;33:6200.
[26] Gatos KG, Kandilioti G, Galiotis C, Gregoriou VG. Polymer 2004;45:4453.
[27] Guadagno L, Naddeo C, Vittoria V. Macromolecules 2004;37:9826.
[28] Rosa CD, Ballesteros OR, Santoro M, Auriemma F. Polymer 2003;44:6267.
[29] Zhu XY, Yan DY, Yao HX, Zhu PF. Macromol Rapid Commun 2000;21:354.
[30] Hanna LA, Hendra PJ, Maddams W, Willis HA, Zichy V, Cudby MEA. Polymer 1988;29:1843.
[31] Suter UW, Flory PJ. Macromolecules 1975;8:765.
[32] Hsu SL, Hahn T, Suen W, Kang S, Stidham HD. Macromolecules 2001;34:3376.